V
BB

GSI

GSI-Preprint-96-27
JUNI 1996

TWO-PHONON GIANT DIPOLE RESONANCE IN 208Pb

K. BORETZKY, J. STROTH, E. WAJDA, T. AUMANN, TH. BLAICH, J. CUB,
TH.W. ELZE, H. EMLING, W. HENNING, R. HOLZMANN, H. KLINGLER,
R. KULESSA, J.V. KRATZ, D. LAMBRECHT, Y. LEIFELS, E. LUBKIEWICZ,
K. STELZER, W. WALUS, M. ZINSER, E. ZUDE

(Accepted for publication in Physiks Letters B)

Gesellschaft für Schwerionenforschung mbH
Postfach 110552 · D-64220 Darmstadt · Germany

Two-Phonon Giant Dipole Resonance in ^{208}Pb

K. Boretzky[1], J. Stroth[1], E. Wajda[2,3], T. Aumann[4], Th. Blaich[4], J. Cub[2], Th.W. Elze[1], H. Emling[2], W. Henning[5], R. Holzmann[2], H. Klingler[1] R. Kulessa[3], J.V. Kratz[4], D. Lambrecht[4], Y. Leifels[2], E. Lubkiewicz[3], K. Stelzer[1], W. Walus[3], M. Zinser[2], and E. Zude[2]
(LAND Collaboration)

[1] Institut für Kernphysik, Universität Frankfurt, D-60486 Frankfurt, Germany
[2] Gesellschaft für Schwerionenforschung, D-64291 Darmstadt, Germany
[3] Institute of Physics, Jagiellonian University, PL-30-059 Krakow, Poland
[4] Institut für Kernchemie, Universität Mainz, D-55029 Mainz, Germany
[5] Argonne National Laboratory, Argonne, IL 60439, USA

Pacs numbers: 24.30.Cz, 25.70.De, 25.75+r
Keywords: Two-Phonon Giant Dipole Resonance, Electromagnetic Excitation, Decay

Abstract

Excitation of the two-phonon isovector giant dipole resonance was observed in ^{208}Pb projectiles incident on different target nuclei (C, Sn, Ho, Pb, U) at high energy (640 A·MeV). Evidence is found for a two-step electromagnetic excitation mechanism. An enhancement of 1.33(16) for the excitation cross section is observed relative to the harmonic approximation. Neutron- and γ-decay probabilities are derived as well.

The electromagnetic excitation of two-phonon states of giant resonances in heavy-ion collisions at energies far above the Coulomb barrier has attracted considerable interest during the past years [1,2]. In contrast to pion double charge exchange reactions, which led to the discovery of the double-phonon giant dipole resonance [3], the observed cross sections are large, on the order of several hundreds of millibarns. While the distribution of the double isovector giant dipole resonance strength was found to be compatible with that expected in the harmonic approximation, i.e. that of two identical and non-interacting phonons, a somewhat puzzling situation evolved with regard to the magnitude of the total excitation cross sections. Relative to the harmonic limit, cross sections were found to be enhanced by factors of 2 - 3 for ^{136}Xe [4] and ^{197}Au [5] and, under certain assumptions, similar effects seemed to be seen in the doubly magic nucleus ^{208}Pb [6,7]. Whether the enhancement results from unexpected nuclear structure effects, i.e. considerable anharmonicities, or from an imperfect description of the excitation process (e.g. using semi-classical methods) remained so far unexplained [2]. As the two-phonon states represent elementary nuclear excitation modes, a clarification seems mandatory. In peripheral heavy-ion collisions, double giant resonances should predominantly be excited in a sequential two-step electromagnetic process, the strength of which depends on the nuclear charge of the reaction partner, in a manner distinctly different from that of single-step excitation modes. A systematic measurement using different targets, as performed in the present work, should allow to clarify the dynamics of the excitation processes and, in turn, nuclear structure aspect.

A number of targets spanning a wide range in nuclear charge Z_T was bombarded with ^{208}Pb projectiles of 640 MeV per nucleon kinetic energy; the ion beam was delivered by the SIS facility of GSI, Darmstadt. We used natural U (238 mg/cm^2), Pb (256 and 798 mg/cm^2), Ho (800 mg/cm^2), Sn (500 mg/cm^2), and C (180 mg/cm^2) as target materials, and an additional run was performed without target. The incident beam ions were monitored by two thin plastic scintillation detectors which provided time-of-flight and position information; beam halos were eliminated by means of a vetoing plastic scintillation counter. The excitation energy E^* of the ^{208}Pb projectiles was derived from an invariant-mass analysis, i.e. by measuring the Lorentz invariant quantity $|\sum_i \mathbf{P}_i| = M_P + E^*$ (M_P denotes the projectile rest mass and $\mathbf{P}_i$ the 4-momenta of the projectile dissociation products labelled by the index i). Charged-particle decay of giant resonances in ^{208}Pb is known to be strongly suppressed and thus only neutron decay channels need to be considered (the small direct γ-decay branch is discussed later). After neutron emission, the residual heavy fragment can still be in an excited state, the energy of which is released in subsequent γ decays. To a good approximation, this can be taken care of by adding the total measured γ-ray energy (after transformation into the projectile rest frame) to the invariant mass, which is evaluated using ground-state masses.
The principle of the procedure and the experimental technique have already been described earlier [4]. Here the set-up was slightly modified and improved. The nuclear charge Z_F of the heavy projectile fragment, deflected in a dipole magnet of

large aperture (1.6 m x 0.5 m), was identified by means of an energy-loss measurement in an ionisation chamber with a resolution of 0.8 e (all resolutions are quoted as FWHM). Since solely neutron decay channels were of interest, only fragments of a nuclear charge $Z_F = 82$ were accepted in the analysis. The fragment momentum was obtained from position measurements in two multi-wire proportional counters (resolution $\sim$ 1.6 mm) and a velocity measurement using two thin plastic scintillators which deliver time of flight information. From the latter a resolution of 0.003 c for the fragment velocity v $\approx$ 0.80 c was obtained.
Neutrons emitted from the excited ^{208}Pb projectiles were detected in LAND, the Large Area Neutron Detector, described in detail in [8]. This detector has an active area of 2x2 m^2 and was placed 11.4 m downstream from the target, centered around the beam axis. Neutron momenta were obtained from the position of incidence on LAND and from time of flight between the target and LAND. Internal calibrations for time and position were derived from an analysis of cosmic-ray tracks, resulting in an average position resolution of 7 cm and a time resolution of 460 ps. The absolute time of flight calibration is achieved using energetic γ rays emerging from central collisions in the target, to which LAND is sensitive as well. The response of LAND with regard to neutrons was studied previously [9], using neutrons of well defined energy obtained from deuteron break-up. For the present experiment the single-neutron detection efficiency amounted to 94(2)%. Neutrons impinging onto LAND lead to extended showers of charged particles, which in case of multiple hits can overlap. To resolve them, a specific pattern recognition algorithm was developed and its capability was studied in detail on the basis of the neutron calibration data and employing a neutron event-mixing procedure [10].
An array of 66 BaF_2 scintillators arranged in the forward hemisphere served to observe γ rays released from the excited residual fragment. The performance of the γ detector was studied extensively by Monte Carlo simulations using the GEANT transport code [11]. As a result, we found that, due to incomplete energy deposit in the detector and its limited solid angle coverage, on the average only about 30-40% of the total γ-ray energy is detected. For the present experiment this leads to an average missing excitation energy of up to 3 MeV (see below).
The invariant-mass analysis finally resulted in differential cross-section distributions $d\sigma/dE^*$ composed of one to three neutron-decay channels; higher neutron multiplicities were found to be negligible. The spectra were subject to several corrections, such as finite efficiencies or solid-angle coverage (see also [4]). Background arising from interactions outside the target, mainly in the fragment detectors or in air, was subtracted on the basis of the measurement without target. Contributions to the differential cross section stemming from nuclear interactions between target and projectile were determined from the cross section observed for the lightest target, i.e. carbon (for which electromagnetic excitation is negligible), adopting an $A_T^{1/3}$ dependence of peripheral reactions (A_T = target nuclear mass) as discussed in detail in [5]. As examples, we show in Fig.1 differential cross sections $d\sigma/dE^*$ obtained with the Pb and Sn targets.
The correction for the spectra just described do not remove all of the experimental

bias, in particular those due to the deficiencies in the neutron multiple-hit recognition and due to the incomplete γ detection discussed above. Such effects cannot be unfolded in a simple manner. A major effort, therefore, was made to implement an 'instrumental filter', which calculated cross-section distributions had to pass prior to comparison with the experimental data [10]. This was accomplished by using the measured response of LAND to neutrons and the GEANT simulations for the γ detection (see above). Therein, the de-excitation process, i.e. neutron and subsequent γ decay, is described assuming a statistical decay with parameters chosen as close as possible to the present experiment. These simulations reveal resolutions with regard to the excitation energy of 2-6 MeV, increasing with excitation energy, and non-linearities of up to 3 MeV. Most striking is the missing energy due to the incomplete γ detection, which can be seen as a shift in excitation energy, e.g. in Fig.1, when comparing the calculated distributions (see below) before and after convolution with the instrumental filter (solid lines in top and middle panel of Fig.1).

The measured cross sections $d\sigma/dE^*$ were compared to cross-section predictions for the electromagnetic excitation processes, calculated in the semi-classical approach developed by Winther and Alder [12] for energetic but distant heavy-ion collisions. For input we used strength distributions for the isovector giant dipole resonance (GDR) and isoscalar and isovector quadrupole resonances (GQR) from the literature, while the unknown cross-section distribution of the double-phonon giant dipole resonance (DGDR) was parameterized. Excitations of higher-multipole resonances and other multi-step excitations (e.g. quadrupole-quadrupole) can be neglected. The strength distribution for the GDR in ^{208}Pb is well known from photo-neutron data. Vessiére et al. [13] have parameterized it by a single lorentzian distribution with a resonance energy of 13.4 MeV and a width of 4.0 MeV. We adopted, however, a more sophisticated parameterization in terms of three truncated lorentzian shapes, comprising a strength of 122% of the TRK sum rule, provided in [14]. For the isoscalar and isovector giant quadrupole resonances we used parameters which we extracted as weighted mean values from the data compiled in [15,16,17 and citations therein]; the data for the isovector GQR, however, are less precise. Examples for semi-classical cross-section calculations using these strength distributions are shown in Fig.1; the distributions are dominated by the GDR excitation, while each of the GQR's contributes only about 10% to the total observed cross section. Uncertainities in the isovector GQR parameters were found to have no significant influence on the DGDR results presented below. For the cross section of the DGDR we chose a parameterization with a gaussian distribution, having in mind that the one-phonon lorentzian distribution appears to be truncated both at its low-energy side because of depletion of strength [18] and at its high-energy side because of the excitation mechanism ('adiabatic cutoff').
The semi-classical method involves an integration over the impact parameter. Following the arguments in [19] we chose a sharp-cutoff approximation for the minimum impact parameter b_{min} and used the description suggested in [20] for its dependence on target and projectile mass.

The calculated distributions in $d\sigma/dE^*$ composed of the above-mentioned components are compared to the experimental ones, thereby determining the following free parameters in a least-squares minimization: mean energy and width of the DGDR cross section with a gaussian distribution and constrained to be the same for all targets (i.e. Sn, Ho, Pb, U), the magnitude of the DGDR cross section for each target, and a renormalisation of the one-phonon cross section for each target. Prior to comparison with the experimental spectra, the calculated cross-section distributions were passed through the instrumental filter (see above). In the error estimation for the various quantities deduced below we have taken into account correlations between the fitted parameters as well as uncertainities of data adopted from literature. From this analysis, we draw conclusions outlined below. Therein, we make use of the independent-phonon model as a reference for the observed DGDR quantities. In each case, the 'harmonic' quantities of the DGDR are calculated from corresponding values of the single GDR, which were known or were determined in this experiment as well.

One-phonon excitations:

(i) As seen from Fig.1, at excitation energies relevant for the single GDR and GQRs ($E^* \leq$ 25 MeV) the experimental spectra are nearly perfectly reproduced by the calculated ones. In the upper part of Fig.2 we show the cross sections[1)], integrated over excitation energy $E^*(0 \leq E^* \leq 40$ MeV), for the one-phonon GDR in comparison to the values calculated in the semi-classical approach[2)]. Averaging over the measurements with different targets we find a renormalisation factor of 1.01 (2) for the single-step excitations, consistent with unity. This finding gives confidence, both to the semi-classical method and the procedure of analysis. Moreover, the parametrization for b_{min} of [20] is confirmed, as this is the only free parameter to determine the target dependence of the integrated cross sections.

Two-phonon giant dipole resonance:

(ii) The integrated cross sections[1)] for the two-phonon giant dipole resonance are also shown in Fig.2 as function of the target nuclear charge Z_T. The dependence on Z_T is distinctly different from that of the one-phonon cross section. Cross sections from an n-step electromagnetic excitation process should be proportional to $Z_T^{n\cdot(2-\delta)}$ (δ reflects a small correction to the usual Z_T^2 dependence of a single-step process which results from the impact parameter cut-off b_{min} in the integration [5]).

Thus, if one compares in a doubly logarithmic presentation the slope of one- and two-phonon cross sections with regard to Z_T, one expects a ratio of 1:2. Experimen-

[1]The cross sections measured in this experiment are corrected for the small unobserved γ-decay branch which is discussed in (v) and (vi).

[2]In the semi-classical calculations we make use of the exact solution for the excitation of an harmonic oscillator (see [19], [21], and citations therein).

tally, we observe consistently a ratio of 1:1.8(3). Thus we obtain for the first time a direct proof that the structure assigned to the DGDR in fact arises from a two-step electromagnetic excitation process.

(iii) In the lower part of Fig.2 we show the ratio of the measured integrated DGDR cross sections relative to the ones calculated in the harmonic limit. On the average, a value $\sigma^{\mathrm{DGDR}}/\ \sigma^{\mathrm{DGDR,harm.}} = 1.33(16)$ is obtained for ^{208}Pb investigated here. Although still significantly deviating from unity, the ratio is much smaller than found in earlier experiments for other nuclei, as discussed in the introduction. As usual, we have calculated $\sigma^{\mathrm{DGDR,harm.}}$ following the prescription given in [21] which basically involves a folding of the single-phonon GDR strength by itself. A more elaborate treatment employing the coupled-channels formalism was presented by C. Bertulani et al. [19] and applied to one of our collision systems (^{208}Pb*+Pb, 640 A·MeV). Various effects such as Coulomb-nuclear interferences, single-step excitations of E2 multipolarity into the DGDR and others were investigated therein, but are to small to account for the cross section enhancement observed in this experiment.

(iv) With the gaussian parameterization for the DGDR cross-section distribution, we deduce a peak energy of 26.0(1.3) MeV and a width (FWHM) of 12(5) MeV. While the former value agrees with the value 25.6(0.9) MeV measured by Ritman et al. [6], a lower value for the width of 5.8(1.4) MeV is reported there. The two values, nevertheless, still overlap within errors.
It should be noticed that the electromagnetic excitation process slightly distorts the resonance strength distributions. Small corrections, which can be estimated reliably, need to be applied in extracting e.g. the resonance peak energy or the resonance width from measured cross section distributions. Taking into account such corrections, we deduce for the DGDR a resonance peak energy of 26.6(0.8) MeV and a resonance width of 6.3(1.3) MeV as weighted mean values from this experiment and [6]. In the harmonic limit one would expect twice the corresponding values of the one-phonon state, i.e. 26.8 and 8.0 MeV, respectively. As noticed earlier [1,2], however, the DGDR width in most cases was found to be much closer to a value obtained by multiplying the GDR width with a factor $\sqrt{2}$, which for ^{208}Pb yields 5.7 MeV.

(v) In [6], the cross section for the DGDR excitation followed by double γ decay back to (or into the vicinity of) the groundstate (g.s.) via the one-phonon intermediate state was measured in a similar collision system ^{208}Pb+Bi (1 A·GeV). A value for the direct γ decay of the single GDR into the groundstate was also measured.
Strictly speaking, the experiment performed in [6] measures the quantitites $\sigma \cdot T_{(2)\gamma}/T_{total}$, while our measurement determines $\sigma \cdot T_n/T_{total}$ (σ, $T_{(2)\gamma}$, T_n, and T_{total} denote the excitation cross section, (double) γ-, neutron-, and total decay probabilities, respectively). By combining the results of both experiments, we can

thus deduce the decay branching ratio $BR_{(2)\gamma-n} = T_{(2)\gamma}/T_n$. For that purpose, however, we need to scale cross sections from our measurement to that of the system investigated in [6]. This is accomplished on the basis of semiclassical calculations. As the resulting scaling factor is close to unity, it cannot cause a significant error. For the single GDR, we obtain a decay branching ratio

$$BR_{\gamma-n}^{\mathrm{GDR}} = T_{\gamma}^{GDR}/T_{n}^{\mathrm{GDR}} = 0.019(2),$$

which is consistent with the value of 0.017 from an earlier independent measurement [22]. For the DGDR we deduce a branching ratio

$$BR_{2\gamma-n}^{\mathrm{DGDR}} = T_{2\gamma}^{\mathrm{DGDR}}/T_{n}^{\mathrm{DGDR}} = 4.5\ (1.5)\cdot 10^{-4}.$$

If the assumption of non-interacting phonons is valid, the two phonons forming the DGDR should have identical decay properties. Consequently, in this harmonic limit one would expect $BR_{2\gamma-n}^{\mathrm{DGDR,harm}} = (BR_{\gamma-n}^{\mathrm{GDR}})^2$. From the above numbers we obtain

$$BR_{2\gamma-n}^{\mathrm{DGDR}}/BR_{2\gamma-n}^{\mathrm{DGDR,harm}} = 1.25\ (40),$$

which is consistent with unity within error.

(vi) Finally, we notice that both, the excitation cross section σ^{DGDR} and the double-γ decay probability $T_{2\gamma}^{\mathrm{DGDR}}$, reflecting inverse processes, are governed by the same electric transition probabilities B(E1; g.s. $\leftrightarrow$ GDR) $\cdot$ B(E1; GDR $\leftrightarrow$ DGDR). This is certainly valid for the direct γ-decay from the giant resonance doorway states, and in [22] it was shown that the direct γ-decay from the doorway state is predominant over that from compound states reached after damping, at least for the single-phonon dipole resonance. Using the result derived in (iii) we may thus assume that

$$T_{2\gamma}^{\mathrm{DGDR}}\ /\ T_{2\gamma}^{\mathrm{DGDR,harm.}} \approx \sigma^{\mathrm{DGDR}}/\sigma^{\mathrm{DGDR,harm.}} = 1.33(16).$$

In turn, by combining this with the result of (v), we can derive the neutron-decay probability with respect to its harmonic value amounting to

$$T_{n}^{\mathrm{DGDR}}\ /\ T_{n}^{\mathrm{DGDR,harm.}} = 1.06\ (35).$$

This value represents a remarkable result, since it indicates that, essentially, each of the two phonons decays into the same reservoir of non-resonant states, although the double-phonon giant resonance is embedded into a continuum of much higher level density in comparison to its one-phonon state.

In Table 1, we summarize the experimental parameters which represent presently our best knowledge of the double giant dipole resonance in ^{208}Pb. In Fig.3, we compare these values with the expected values in the harmonic limit.

In summary, we have shown that the process of electromagnetic excitation in energetic heavy ion collisions can be described quantitatively with semi-classical methods. The double giant dipole resonance is observed as an additional cross section on top of one-phonon dipole and quadrupole resonances and the expected two-step excitation mechanism could be verified. Various parameters for the two-phonon giant dipole resonance in ^{208}Pb, such as resonance peak energy and width, excitation cross sections and decay probabilities could be determined and were compared with the independent-phonon model. Contrary to findings for other nuclei, these parameters deviate only slightly, typically on a 10-30% level, from those expected in the harmonic limit. It is conceivable that anharmonicities become more pronounced in the open-shell nuclei studied earlier.

This work was supported by the German Federal Minister for Research and Technology (BMBF) under Contracts 06 OF 474 and 06 MZ 476 and by GSI via Hochschulzusammenarbeitsvereinbarungen under Contracts OF ELZ, MZ KRK and partly supported by the Polish Committee of Scientific Research under Contract PB2/P03B/113/01.

References

1) P. Chomaz and N. Frascaria, Phys. Rep. 252 (1995) 275
2) H. Emling, Part. Prog. Nucl. Phys. 33 (1994) 629
3) S. Mordechai and C.F. Moore, Int. Journal Mod. Phys. E3 (1994) 39
4) R. Schmidt et al., Phys. Rev. Lett. 70 (1993) 1767
5) T. Aumann et al., Phys. Rev. C47 (1993) 1728
6) J.L. Ritman et al., Phys. Rev. Lett. 70 (1993) 533 and 2659
7) J.R. Beene et al., Nucl. Phys. A569 (1993) 163c
8) Th. Blaich et al., N.I.M. in Physics Research A314 (1992) 136
9) J. Cub et al., GSI Scientific Report (1994) 275
10) K. Boretzky, PhD thesis, Universität Frankfurt, Germany (1996)
11) R. Brun et al., GEANT3, Report No. CERN/DD/ec/84-1 (1986)
12) A. Winther and K. Alder, Nucl. Phys. A319, (1979) 518
13) A. Vessiére et al., Nucl. Phys. A159 (1970) 561
14) K.P. Schelhaas et al., Nucl. Phys. A489 (1988) 189
15) D.S. Dale et al., Phys. Rev. Lett. 68 (1992) 3507
16) F.E. Bertrand et al., Am. Rev. Nucl. Sci. 26 (1976) 457
17) A. v. Woude, Int. Rev. of Nucl. Phys. 7, (1991) 100
18) J. Kopecky and M. Uhl, Phys. Rev. C41 (1990) 1941
19) C.A. Bertulani et al., Phys. Rev. C53 (1996) 334
20) C.J. Benesh et al., Phys. Rev. C40 (1989) 1198
21) W. Llope and P. Braun-Munzinger, Phys. Rev. C41 (1990) 644 and Phys. Rev. C45 (1992) 799
22) J.R. Beene et al., Phys. Rev. C41 (1990) 920

Tab. 1: Experimental values for the resonance peak energies E_o, resonance width Γ, (double) γ- to neutron-decay branching ratios $T_{(2)\gamma}/T_n$ and integrated ($0 \leq E^* \leq 40$ MeV) excitation cross sections σ for the single (GDR) and double (DGDR) isovector giant dipole resonance in ^{208}Pb. The cross sections are listed for targets U, Pb, Ho, and Sn.

		GDR	DGDR
σ [b] [1]	U	3.66 (11)	0.51 (9)
	Pb	3.28 (5)	0.38 (4)
	Ho	2.47 (5)	0.28 (5)
	Sn	1.45 (5)	0.07 (3)
E_o[MeV]		13.4 [2]	26.6(8) [3]
Γ [MeV]		4.0 [2]	6.3(1.3) [3]
$T_{(2)\gamma}/T_n$ [4]		0.019(2)	$4.5(1.5)\cdot 10^{-4}$

[1] from this experiment for the ^{208}Pb beam (640 A·MeV) on targets as indicated
[2] from [13]
[3] weighted mean value from this experiment and [6]
[4] from combined data of this experiment and [6]

Fig. 1: (upper panel): Calculated cross sections $d\sigma/dE^*$ obtained for the electromagnetic excitation of ^{208}Pb (640 A·MeV) in a Pb target using known strength distributions for the single isovector dipole resonance (dashed line) and sum of isoscalar and isovector quadrupol resonances (dotted line). Cross sections for the double giant dipole resonance as fitted to the experimented data (see text), are given by the dashed-dotted line. The sum of all contributions is shown as solid line.
(middle panel): Measured differential cross sections $d\sigma/dE^*$ for ^{208}Pb (640 A·MeV) excited in a Pb target and the corresponding calculated distribution (solid line), obtained from applying the experimental filter to the cross section shown as solid line in upper panel.
(lower panel): same as in the middle panel however, for a Sn target.

Fig. 2: (upper panel): Integrated experimental cross sections for the one-phonon isovector giant dipole resonance and the two-phonon dipole resonance in ^{208}Pb obtained from different targets of nuclear charge Z_T. The dashed lines interpolates cross-section predictions from the semi-classical calculation (see text); in case of the DGDR, the calculated values are multiplied by a factor of 1.33.
(lower panel): Ratio of the experimental cross sections for the DGDR in ^{208}Pb to the ones calculated in the harmonic approximation for different targets. The mean value and its error are indicated by solid and dashed lines, respectively.

Fig. 3: Comparison of various experimental quantities X for the two-phonon giant dipole resonance (DGDR) in ^{208}Pb with those obtained in the harmonic limit $X^{harm.}$. Results are shown for the resonance peak energy E_o, width Γ, integrated cross section σ (averaged over all targets), decay branching ratio $T_{2\gamma}/T_n$ and neutron decay probability T_n. In all cases, the harmonic values $X^{harm.}$ are obtained using the known values of the single GDR.

– Fig. 1 –

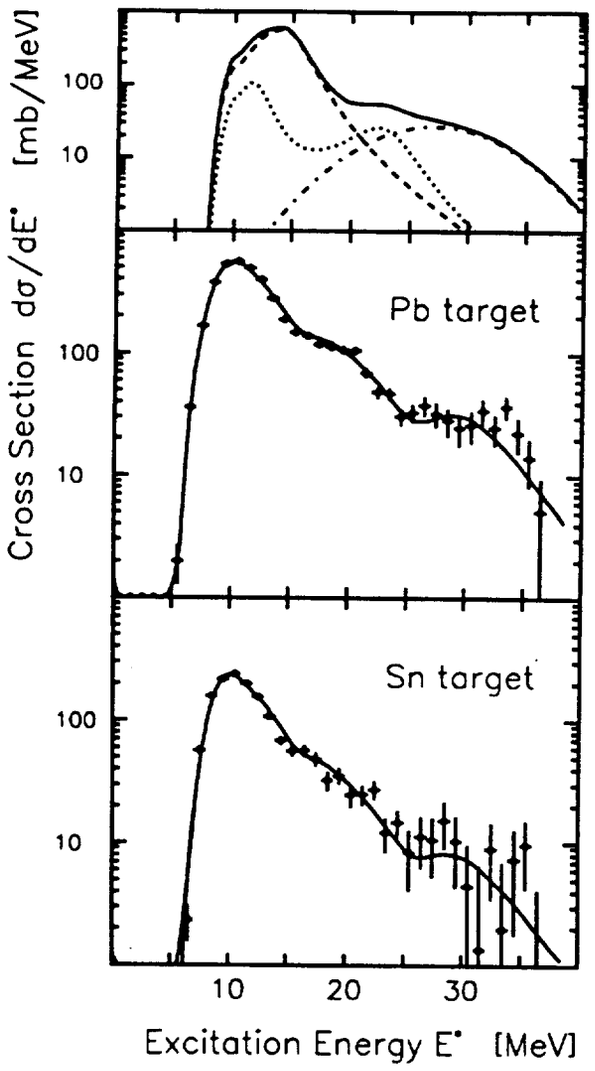

– Fig. 2 –

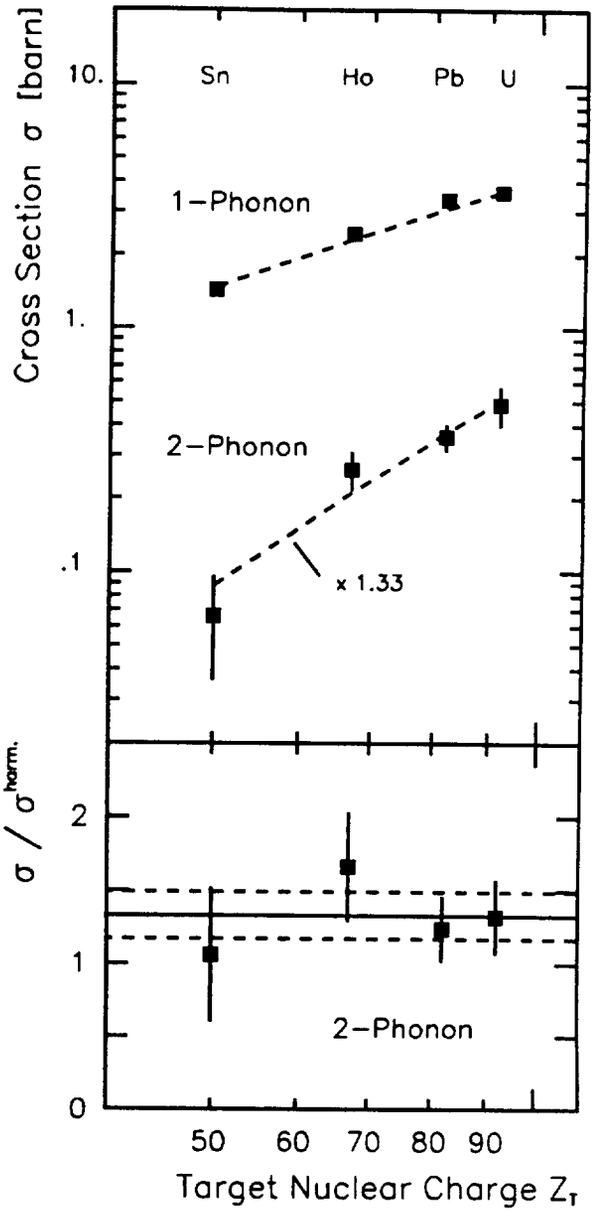

– Fig. 3 –